LA-UR-20-22242
Approved for public release; distribution is unlimited.

Title:	Mitigation of Beam Losses in LANSCE Linear Accelerator
Author(s):	Batygin, Yuri Konstantinovich
Intended for:	International Committee for Future Accelerators (ICFA) Beam Dynamics Newsletter
Issued:	2020-03-10

1.1 Mitigation of Beam Losses in LANSCE Linear Accelerator

Yuri K. Batygin
Mail to: batygin@lanl.gov
Los Alamos National Laboratory, Los Alamos NM 87545 USA

1.1.1 Introduction

Suppression of beam losses is essential for successful operation of high-intensity accelerator facility. The LANSCE accelerator started routine operation in 1972 as a 0.8 MW average proton beam power facility for meson physics research, and delivered high-power beam for a quarter century [1]. The accelerator currently delivers 100 MeV proton beam to Isotope Production Facility (IPF) and 800 MeV H^- beams to various experimental areas (see Figure 1 and Table 1). The accelerator is equipped with two independent injectors for H^+ and H^- beams, merging at the entrance of a 201.25 MHz Drift Tube Linac (DTL). The DTL performs acceleration up to the energy of 100 MeV. After the DTL, the Transition Region beamline directs a 100 MeV proton beam to the Isotope Production Facility, while the H^- beam is accelerated up to the final energy of 800 MeV in an 805-MHz Coupled Cavity Linac. The H^- beams, created with different time structure by a low-energy chopper, are distributed in the Switch Yard (SY) to four experimental areas: the Lujan Neutron Scattering Center equipped with a Proton Storage Ring (PSR), the Weapons Neutron Research facility (WNR), the Proton Radiography facility (pRad), and the Ultra-Cold Neutron facility (UCN). Multi-beam operation requires careful control of accelerator tune to minimize beam losses [2]. In this paper we review main effects affecting beam losses in LANSCE linear accelerator and discuss methods to reduce them.

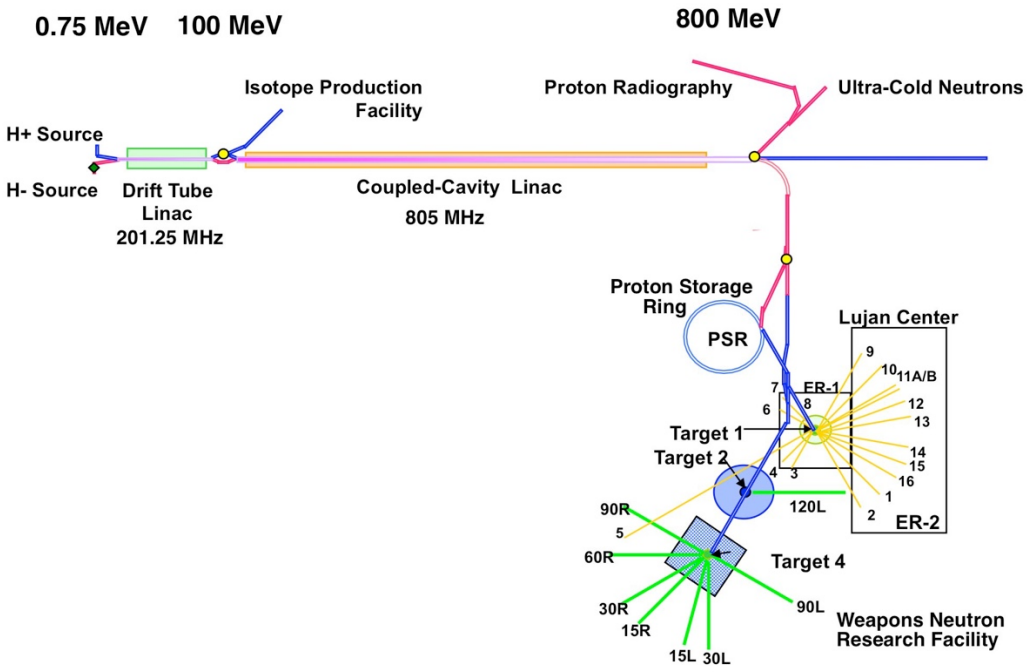

Figure 1: Layout of LANSCE Accelerator Facility.

Table 1: Beam parameters of LANSCE accelerator.

Area	Rep. Rate (Hz)	Pulse Length (μs)	Current / bunch (mA)	Average current (μA)	Average power (kW)
Lujan	20	625	10	100	80
IPF	100	625	4	250	23
WNR	100	625	25	4	3.6
pRad	1	625	10	<1	<1
UCN	20	625	10	10	8

1.1.2 **Beam Loss in Accelerator**

Beam losses in the LANSCE accelerator are mainly determined by the two most powerful beams: the 80 kW H^- beam injected into Proton Storage Ring, and the 25 kW H^+ beam, which is used at the Isotope Production Facility. The main sources of beam losses in linac are mismatch of the beam with the accelerator structure, variation and instabilities of accelerating and focusing fields, transverse-longitudinal coupling in the RF field, misalignments and random errors of accelerator channel components, field nonlinearities of focusing and acceleratirng elements, beam energy tails from un-captured particles, particle scattering on residual gas and intra-beam stripping, non-linear space-charge forces of the beam, excitation of high-order RF modes, and dark current from unchopped beams.

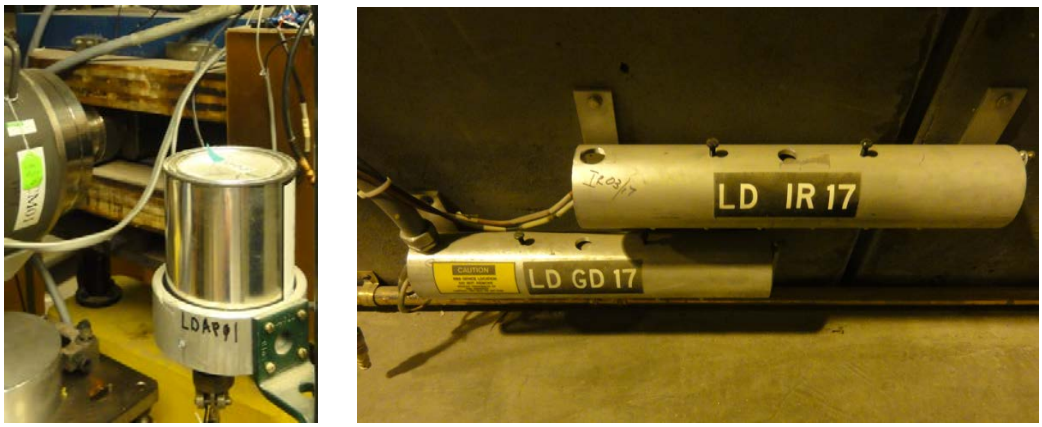

Figure 2: (left) Activation Protection (AP) scintillation detector, (right) Ion Chamber (IR) and Gamma Detector (GD).

The main control of beam losses is provided by Activation Protection (AP) detectors (see Figure 2), which are one-pint size cans with a photomultiplier tube immersed in scintillator fluid. AP detectors integrate the signals and shut off the beam if the beam losses around an AP device exceed 100 nA of average current. Another type of loss monitor are Ion Chamber (IR) detectors, which are used in the high energy transport lines. They are usually located in parallel with a Gamma Detectors (GD) that feeds into Radiation Safety System (see Figure 2). The third type of beam loss monitor are Hardware Transmission Monitors (HWTM). The HWTM system measures the beam current losses between current monitors or can limit beam current to a value at one current monitor. The

typical HWTM constraints of 10 nA/m of accelerator length are aimed to prevent moderate to large beam losses usually occur during accelerator tune-up period or when beamline device malfunctions. Typical distribution of beam losses along accelerator facility after careful beam tuning are presented at Figures 3, 4. Integral losses in high-energy Coupled-Cavity Linac and in Proton Storage Ring are presented in Table 2. Typical averaged beam losses along linear accelerator are 2 x 10^{-3} which corresponds to loss rate of 3 x 10^{-6} m^{-1}, or 0.2 W/m. In high-energy beamlines, total beam loss are 4 x 10^{-3} which corresponds to loss rate of 2 x 10^{-5} m^{-1}, or 1.6 W/m. Higher beam loss in HEBT are explained by dispersive nature of beamlines, which generates additional losses due to longitudinal beam tails and energy tails. Typical average losses in Proton Storage Ring are at the level of 0.3%. Sources and optimization of beam loss in PSR are discussed in details in Ref. [3].

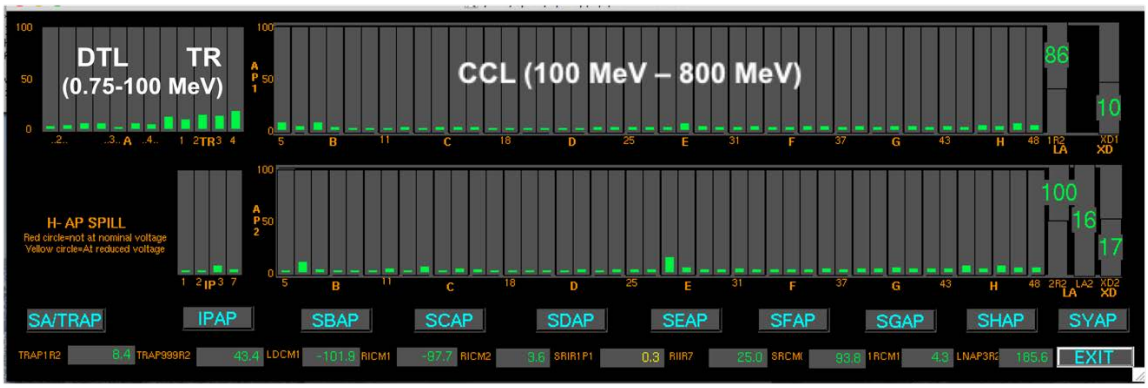

Figure 3: Beam loss along Drift Tube Linac (DTL), Transition Region (TR), and Coupled Cavity Linac (CCL).

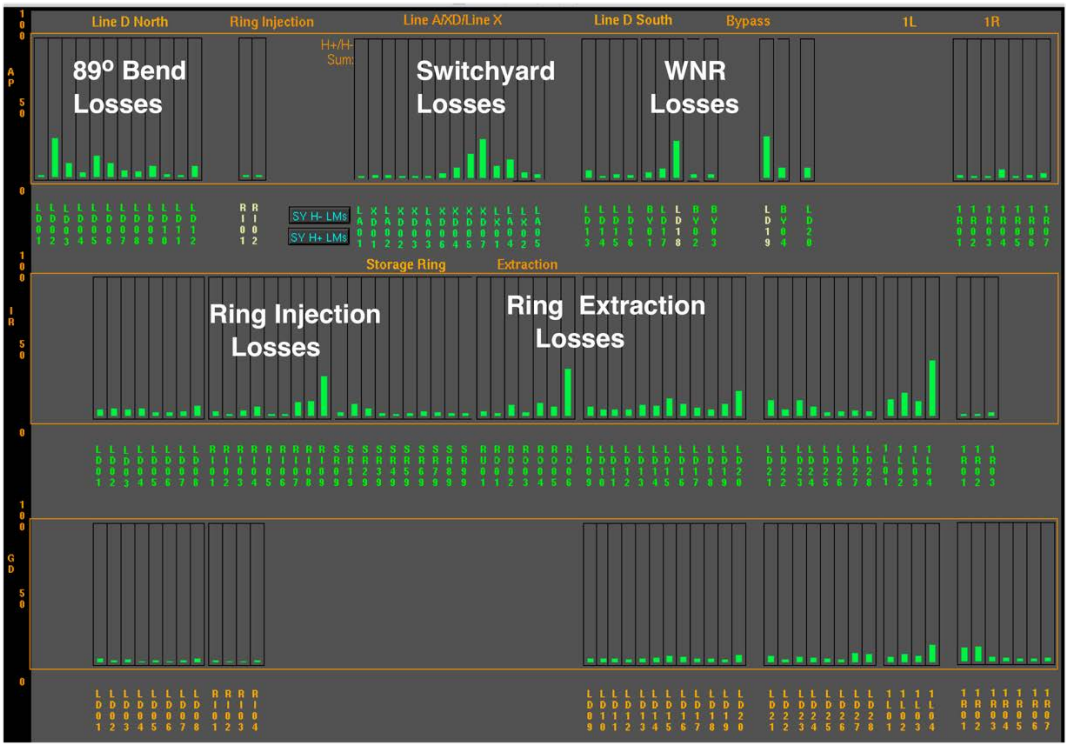

Figure 4: Beam losses in high-energy beam transport.

Table 2: Integral Beam Losses in Accelerator.

Year	Summed Losses in Coupled Cavity Linac (AP reading)	Relative Proton Storage Ring beam losses (%)
2019	140	0.14
2018	180	0.39
2017	150	0.32
2016	190	0.32
2015	135	0.13
2014	211	0.24
2013	190	0.23
2012	183	0.26
2011	167	0.24

1.1.3 **Ion Sources and Low Energy Beam Transport**

Optimal operation of the accelerator facility critically depends on the emittance and brightness of the beam extracted from the ion sources and beam formation in the low-energy beam transport (LEBT). The H^+ beam injector includes a duoplasmatron proton source mounted at 750 keV Cockroft-Walton accelerating column, and low-energy beam transport [4]. Presently the source delivers a proton beam current of 5 mA at 100 Hz x 625 μsec pulse length. Normalized rms beam emittance, ε_{rms}, extracted from a particle source with aperture radius R and plasma ion-temperature T is estimated as

$$\varepsilon_{rms} = \frac{R}{2}\sqrt{\frac{k_B T}{mc^2}}\ , \tag{1}$$

where k_B = 1.38 x 10^{-23} J/K is the Boltzmann constant, and mc^2 is the ion rest energy. Additional sources contributing to beam emittance are irregularities in the plasma meniscus extraction surface, aberrations due to ion-source extraction optics, non-linearity of the electric field created by the beam space charge, beam fluctuations due to ion-source instability or power regulation. Typical value of rms normalized proton beam emittance is ε_{rms} = 0.002 - 0.004 π cm mrad. Optimization of source performance is related to maximization of normalized beam brightness:

$$B = \frac{I}{8\pi^2 \varepsilon_{x\_rms}\varepsilon_{y\_rms}}, \tag{2}$$

where I is the beam current, and ε_{x_rms}, ε_{y_rms} are normalized beam emittances in x- and y -directions. Proton beam brightness is optimized as a function of matching parameter $\eta = P_b / P_o$, which is a ratio of beam perveance, $P_b = I / U_{ext}^{3/2}$, to Child-Langmuir perveance, $P_o = (4\sqrt{2}\pi / 9) S^2 \varepsilon_o \sqrt{q/m}$:

$$\eta = \frac{9}{\sqrt{2}S^2}\frac{I}{I_c}\left(\frac{mc^2}{qU_{ext}}\right)^{3/2}, \tag{3}$$

where $I_c = 4\pi\varepsilon_o mc^3/q = A/Z \cdot 3.13 \cdot 10^7$ [Amp] is the characteristic beam current, U_{ext} is the extraction voltage, $S = R/d$ is the ratio of extraction radius to extraction gap. Study indicates that proton beam brightness is maximized at the value of $\eta \approx 0.52$ (see Figure 5) [5].

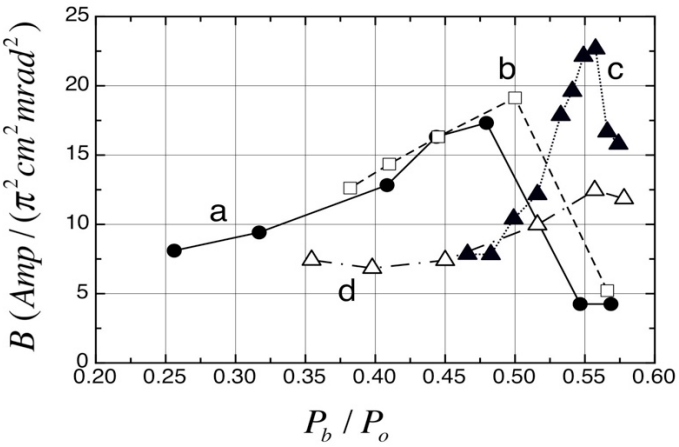

Figure 5: Measured proton beam brightness as function of ratio of beam perveance to Child-Langmuir perveance.

The H- beam injector includes a cesiated, multicusp - field, surface - production ion source [6] with beam current 14 - 15 mA at 120 Hz x 625 μsec and two-stage low-energy beam transport. Normalized beam emittance of this type of source is estimated as the phase space area comprised by a converter with radius R_{conv}, extractor aperture with radius R_{ext}, and distance L_{conv} between them (admittance of source) [7]

$$\varepsilon = \frac{4}{\pi}\sqrt{\frac{2eU_{conv}}{mc^2}}\frac{R_{conv}R_{ext}}{L_{conv}}, \tag{4}$$

where U_{conv} is the voltage between the converter and the source body. In the LANSCE H- ion source, R_{conv} =1.9 cm, R_{ext} = 0.5 cm, L_{conv} =12.62 cm, U_{conv} = 300 V, which yields a normalized beam emittance of ε = 0.076 π cm mrad. This quantity is close to the experimentally observed value of four-rms normalized beam emittance $4\varepsilon_{rms} = 0.07\ \pi$ cm mrad. Beam brightness of H- source is a weak function of extraction voltage (see Figure 6). Beam brightness can be increased through minimization of converter voltage, see Equation (4). Table 3 illustrates increase of H- source beam brightness by 29% via reduction of converter voltage from 275 V to 185 V. Lowering of converter voltage is limited by the voltage (~ 170V) between heated filament cathode and source body for plasma generation. Typical value of converted voltage within operational period is $U_{conv} \approx 250$ kV, which enshures low frequency of source arc-downs, and thus provides long-term stability of source operation. Beam brightness of H- source does not change while extracted beam current increased from 15 mA to 20 mA [8].

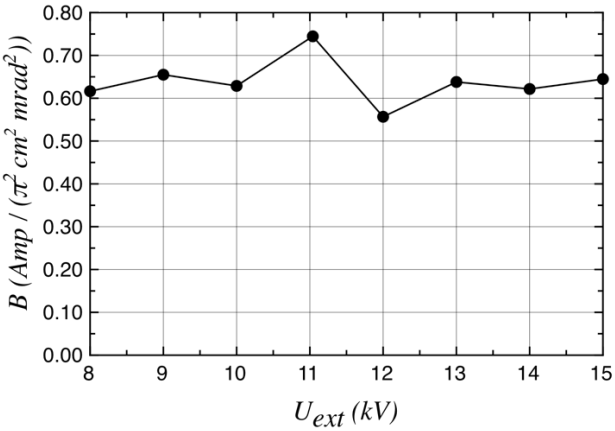

Figure 6: Brightness of H^- source as function of extraction voltage.

Table 3. H^- source beam emittance and brightness.

Converter Voltage U_{conv} (V)	Normalized x - rms beam emittance ε_{x_rms} (π cm mrad)	Normalized y - rms beam emittance ε_{y_rms} (π cm mrad)	Source Current (mA)	Normalized Beam Brightness B [A/(π cm mrad)^2]
275	0.017	0.0166	14.3	0.642
185	0.015	0.0145	14.3	0.832

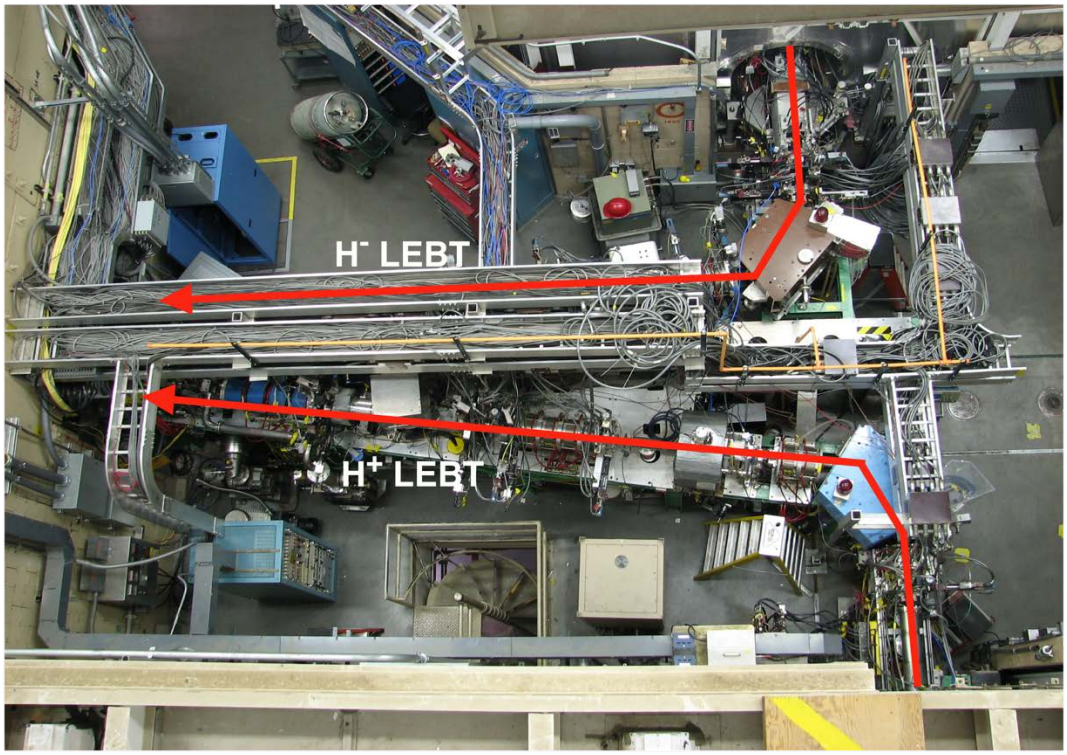

Figure 7: Top view of 750 - keV Low Energy Beam Transports (LEBT) of H^+ and H^- beams.

Both beams are transported in 750 keV beamlines and merged before injection into Drift Tube Linac (see Figure 7). Space charge significantly affect beam dynamics. Space charge factor of depression of transverse oscillations in proton beamline is [9]

$$\frac{\mu}{\mu_o} = \sqrt{1+b_o^2} - b_o , \tag{5}$$

where b_o is the space charge parameter:

$$b_o = \frac{1}{(\beta\gamma)^2}\frac{I}{I_c}\frac{S}{\mu_o(4\varepsilon_{rms})}, \tag{6}$$

μ_o is the phase advance of transverse oscillations per focusing period *S* of the beam with negligible current, and μ is that of the beam with significant current. Space charge neutralization plays an important role in H^- beam dynamics. Typical spectra of residual gas in the 750 keV transport channel indicate that main components are H_2 (48%), H_2O (38%) and N_2 (9%), while residual gas pressure is $5\cdot10^{-7}$ Torr. Emittance scans indicate a significant variation of beam parameters versus beam pulse length due to space-charge neutralization effect (see Figure 8) [10]. The value of space-charge neutralization is defined as

$$\chi = 1 - \frac{I_{eff}}{I}, \tag{}$$

where I_{eff} is the effective beam current under neutralization. Measurements [10] show that space charge neutralization of H^- beam along 750-keV beamline varies between 50% - 90%, while neutralization of H^+ beam does not exceed 20%. For H^- beamline, the space charge parameter is b_o = 0.125, therefore the beam transport is emittance dominated. Correspondingly, the space charge depression factor for H^- beam is $\mu/\mu_o = 0.88$. For proton beam space charge depression factor is $\mu/\mu_o = 0.41$, and dynamics of proton beam is space-charge dominated.

Emittance growth due to space charge is estimated as [11]

$$\frac{\varepsilon_f}{\varepsilon_i} = \sqrt{1 + (\frac{\mu_o^2}{\mu^2} - 1)(\frac{W_i - W_f}{W_o})}, \tag{7}$$

where $(W_i - W_f)/W_o$ is the "free-energy" parameter due to space-charge induced beam intensity redistribution. Both proton and H^- beam have initial distribution between "Water Bag" and parabolic distribution in 4D phase space. Parameter $(W_i - W_f)/W_o$ has a value of 0.01126 for "Water Bag" distribution, and 0.0236 for parabolic beam distribution in 4D phase space. The estimated space charge emittance growth from Eq. (9) is between 3% - 6 % for proton beam and 0.16% - 0.34% for H^- beam. In experiments, no noticeable emittance growth due to space charge were observed for both beams. However, space charge plays a significant role in beam matching to the structure. Knowledge of effective

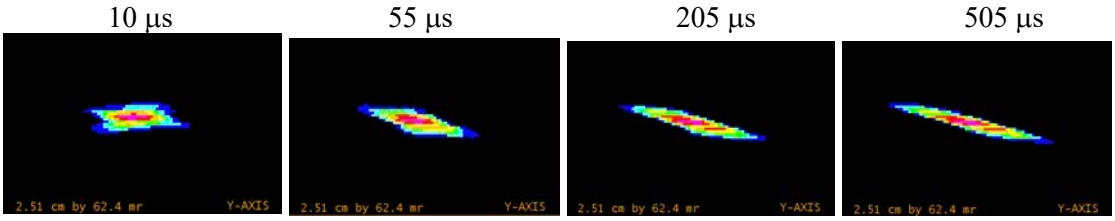

Figure 8: Variation of vertical H^- beam emittance along the beam pulse in 750 -keV LEBT.

beam current under space charge neutralization allows precise beam tuning in the structure. Typical beam losses in each beamline are within 0.5 mA peak current.

Both beams experience emittance growth due to RF bunching. Transverse beam emittance growth crossing a single RF gap is [12]

$$\frac{\Delta\varepsilon}{\varepsilon} = \frac{k^2\beta_w^2}{10}\Phi^2\sin^2\varphi_s\,, \tag{8}$$

where β_w is the value of beam beta Twiss parameter in RF gap, Φ is the phase length of the bunch, φ_s is the synchronous phase of the bunch, and k is the parameter of RF gap with applied voltage U and transit-time factor T of the cavity with wavelength λ:

$$k = \frac{\pi qUT}{mc^2(\beta\gamma)^3\lambda}\,. \tag{9}$$

Relative increase of proton beam emittance is around 1.9, and that of H^- beam is 1.2. Additionally, WNR H^- beam with 36 ns pulse length experiences 30% emittance growth due to chopping.

In 2014, the operation pulse rate of the LANSCE accelerator facility changed to 120 Hz, following a decade-long period of operation at a 60 Hz pulse rate. While working at 60 Hz with 825 μsec pulse length, the H^- source was operated with a 5% duty factor (60 x 0.000825). The source steadily delivered a 16 mA beam within a 28-day operation cycle, reaching a 0.53 A-hour lifetime (0.016 A x 28 days x 24 hours x 0.05 = 0.53 A-hour). Currently, the H^- source operates at the highest-ever possible duty factor of 10%, delivering maximum current of 14 mA within 28 days with a 0.94 A-hour lifetime. After transformation to the double pulse rate, the beam power for the Weapons Neutron Research Facility increased by a factor of 2.5, while the power of other beams remains unaltered.

Historically, it was assumed that the H^- beam is close to being completely space-charge neutralized in the beam transport, and the effective current was assumed to be 1 mA. With the performed study of space-charge neutralization [10], it was found that the value of effective current differs significantly from the expected value of 1 mA. Figure 9 illustrates beam transmission through the beamline tuned using the historically adopted method with an effective beam current of 1 mA, and that with the new approach based on our space-charge neutralization study. Accordingly, it was demonstrated that beam transmission through the beamline has improved significantly with the latter approach. Particularly, the optimization gives rise to the possibility of attaining the same peak output current of 10 mA, with a concurrent decrease of peak source current from 16 mA to 14

mA. The outcome of this improvement is that the Lujan Neutron Scattering Center maintains operation with nominal beam power of 80 kW, while the WNR beam has increased its current by a factor of 2.5.

Operation of H^+ low-energy beam transport indicated that the proton beam emittance growth is mostly determined by misalignment of beamline components. A beam based steering procedure in Low Energy Beam Transport and in IPF beamline was implemented to minimize emittance growth [13]. It included the determination of beam offset and beam angle upon entering a group of quadrupoles, with subsequent correction of beam centroid trajectory to minimize beam offset in a series of quadrupoles. Application of this procedure resulted in significant reduction of emittance growth in proton Low Energy Beam Transport.

Figure 9: Transmission of tuned chopped H^- beam along 750 -keV beam transport: (a) assuming full space charge neutralization, (b) based on actual space charge neutralization. Reduction of beam intensity (80%) between TBCM1 and TBCM2 current monitors is due to beam chopper.

1.1.4 **Beam Dynamics in Drift Tube Linac and IPF Beamline**

The Drift Tube Linac consists of 4 tanks with energies 5 MeV, 41 MeV, 73 MeV, and 100 MeV, respectively. Table 4 illustrates capture efficiency of various beams into DTL. Beam tune is optimized to maximize capture of most powerful H^- Lujan beam at the level of 75% - 80%. Parameters of H^- pRad/UCN beams are similar to that of H^- Lujan beam. Initially 20% - 25% of that beams are lost in the beginning of Tank 1. Proton beam and H^- WNR beam have different phase space characteristics and captured with lower efficiency. Subsequent beam losses of 0.1% - 1% in DTL are determined by un-captured particles and by expansion of phase space volume occupied by the beam. Expansion of beam emittance is performed mainly due to increase of peripheral area, while beam core is changing in smaller rate. H^- beam emittance increase by a factor of 1.8 – 2.3, while H^+ beam emittance increase is a factor of 5-6. These values agree with earlier simulation results [14]. While beam distributions and beam currents are significantly different at the entrance of DTL, distribution of all beams at the end of DTL tend to be the same. It reflects the fact that during acceleration beam tends to occupy all available phase space area.

The significant effect of beam emittance growth at low energy is transverse-longitudinal coupling in RF field. Estimated beam emittance growth due to this process is [9]

$$\frac{\varepsilon}{\varepsilon_o} = 1 + \frac{\Phi}{\tan\varphi_s}\left(\frac{\Omega^2}{4\Omega_{rs}^2 - \Omega^2}\right), \qquad (10)$$

Table 4: Beam Capture in Drift Tube Linac

Beam	Beam Capture (%)
H^- (Lujan/UCN/pRad)	75 -82
H^- (WNR)	45 - 50
H^+ (IPF)	60 - 70
Additional losses	0.1 -1

where Ω is the longitudinal oscillation frequency, Ω_{rs} is the transverse oscillation frequency in presence of RF field. In 201.25 MHz linac $\Phi \sim 1.57$ rad, $\varphi_s \sim 30^o$, $\Omega/\Omega_{rs} \sim 0.75$. Expected emittance growth from Eq. (10) is $\varepsilon / \varepsilon_o = 1.62$.

After the DTL, 100-MeV protons enter the transition region (TR) and continue propagation to the Isotope Production Facility (IPF) beamline (See Figure 10). Operation of TR and IPF beamlines include BPM control of the beam centroid, correction of beam position at the target and control of beam losses at the Activation Protection devices. Typical beam losses in IPF beamline are characterized by summed AP device readings of 15% - 20%, which is equivalent to 1-μA beam losses, or relative beam losses of 4×10^{-3}.

Series of beam development experiments were undertaken to reduce beam losses [13]. Analysis of beam dynamics, using 100-MeV beam emittance scan, indicated that beam envelopes had excessive variation, which was corrected by quadupole setup. Additional improvement of beam quality was achieved with beam realignment of the IPF beamline. A combination of the steering and bending magnets were adjusted to centre the beam through the sequence of quadrupoles. As a result of improved beam matching, the beam losses were reduced and reached 5×10^{-4} (see Figure 11).

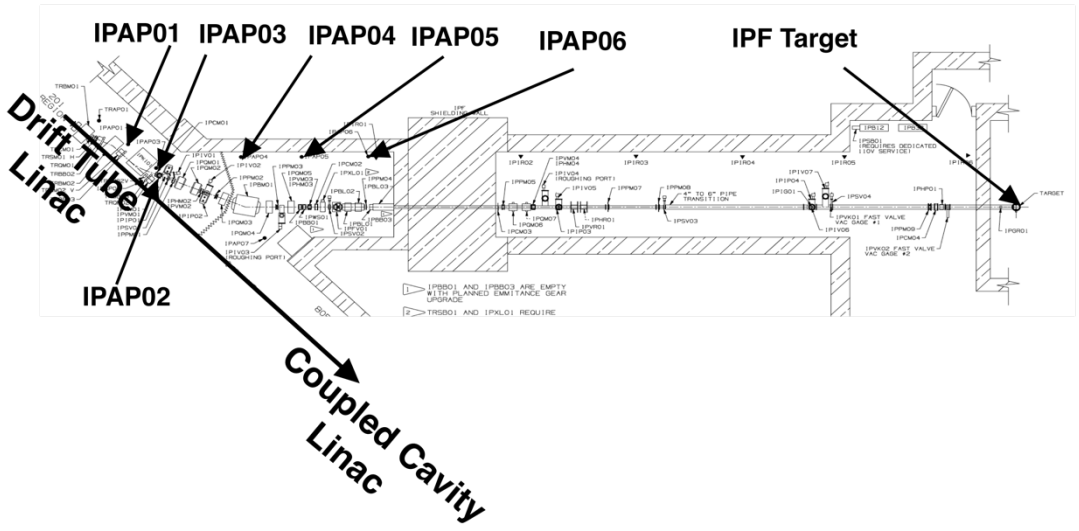

Figure 10: Isotope Production Facility Beamline.

(a)

	H+ %
IPAP01	1
IPAP02	0
IPAP03	14
IPAP04	0
IPAP05	1
IPAP06	2

(b)

	H+ %
IPAP01	0
IPAP02	0
IPAP03	2
IPAP04	0
IPAP05	0
IPAP06	0

Figure 11: Activation protection devices reading (a) before and (b) after retuning.

1.1.5 **Beam Dynamics in Coupled Cavity Linac**

In Coupled Cavity Linac, H^- beam experiences additional emittance growth, and normalized rms beam emittance at the end of linac is 1-5 – 2 larger than that at the beginning of 805 MHz linac. Dominant factor of beam emittance growth in high-energy part of the linac is diffusion of beam distribution on misalignments of accelerator channel, which results in spreading of effective emittance due to coherent perturbation of the beam in presence of frequency dispersion.

Beam losses in high-energy part of accelerator facility are sensitive to selection of amplitudes and phases of 805-MHz linac. Random errors in RF amplitude and phase of accelerating tanks result in rise of amplitude of longitudinal oscillations. Increase of amplitude of relative momentum spread in a sequence of N_a accelerating sections with relative error in RF amplitude $\delta E_o / E_o$, and error in RF phase $\delta\psi$ is estimated as [9]:

$$< \delta(\frac{\Delta p}{p}) >= \sqrt{\frac{N_a}{2}[< \Delta g >^2 + \left(\frac{qE\lambda}{mc^2}\right)\frac{|\sin\varphi_s|}{2\pi\beta\gamma^3} < \delta\psi >^2]}\,, \tag{11}$$

where

$$< \Delta g >= \frac{eE\lambda\cos\varphi_s}{mc^2\beta_N}\sqrt{< \frac{\delta E_o}{E_o} >^2 + tg^2\varphi_s < \delta\psi >^2}\,, \tag{12}$$

$E = E_o T$ is the accelerating gradient, E_o is the average field in the tank, β_N is the average effective beam velocity in linac. The estimation of increase of momentum spread, Eq. (11), indicates that for maximum available instability of the RF field amplitude $< \delta E_o / E_o > \approx 1\%$ and that of phase $< \delta\psi > \approx 1^o$, increase of momentum spread of the beam is around $< \delta(\Delta p / p) > \approx 1.7 \cdot 10^{-4}$, which is a significant addition to regular momentum spread of the beam $\Delta p / p = 8 \cdot 10^{-4}$. The study of beam losses generated by DTL [15] and CCL [16] cavity field errors indicate that to achieve low losses, the stability of the amplitudes and phases should be kept within 0.1% and 0.1°, respectively. Improper tune of accelerator results in appearance of momentum tails in beam distribution (see Figure 12), which generates significant beam spill after accelerator. Precise selection of

amplitudes and phases of high-energy linac are important to minimize beam losses in accelerator facility.

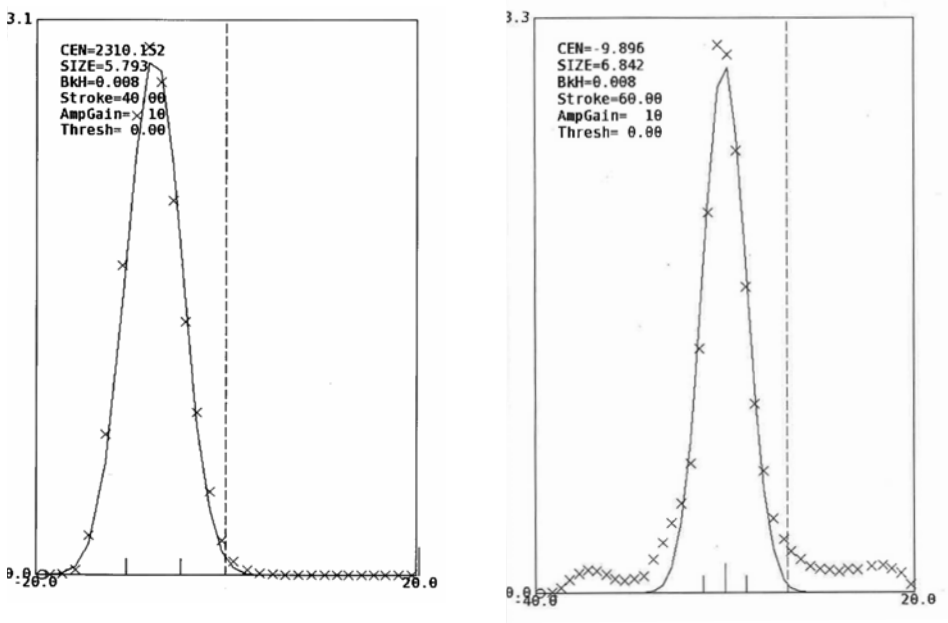

Figure 12: Momentum spread of the beam measured by LDWS03 wire scanner: (left) properly tuned beam, (right) beam with momentum tails due to improper tune.

Beam tuning to LANSCE linear accelerator includes independent transverse and longitudinal matching of the beam to the structure. Transverse matching of the beam is performed through adjustments of beam ellipses in 4D phase space with accelerator lattice using matching quadrupoles. Focusing structure of 805-MHz linac is a FDO structure. Doublets of focusing-defocusing quadrupoles are located between accelerating tanks. Matching is performed using four quadruoles TRQM5-8 in 100-MeV Transition Region between DTL and CCL. Design of quadrupole structure assumes ramp of quadrupole gradient values between modules 5-13 within energy range of 100 - 226 MeV. Experience indicates that beam losses are sensitive to ramp of quadrupole values. Figures 13, 14 indicate significant reduction of beam losses in linac while empirical change of quadupole setups. After module 13 the values of quadrupole gradients are kept constant.

The values of the field amplitudes and phases of the 201-MHz Drift Tube Linac are selected through absorber-collector phase scans, while that in 805-MHz side-coupled linac modules are maintained using a classical “delta-t” procedure [17]. This turn-on method is based on measurement of difference in time of flights between two pairs of pickup loops when accelerating module is off and on, and compare these differences with design differences. Delta-t tuning procedure works well when particles perform significant longitudinal oscillations within RF tanks. With increase of beam energy, longitudinal phase oscillations adiabatically damped, and accuracy of delta-t method drops.

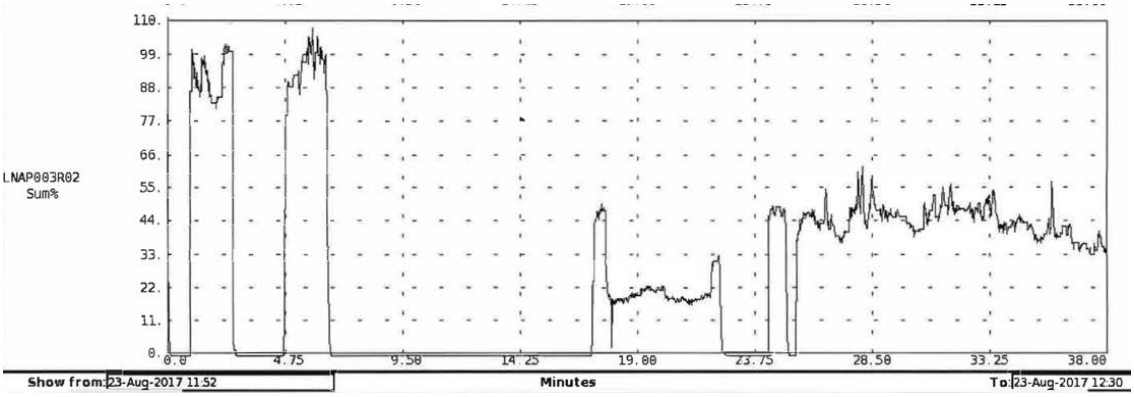

Figure 13: Reduction of sum beam losses in 805-MHz linac through change of quadrupole ramp.

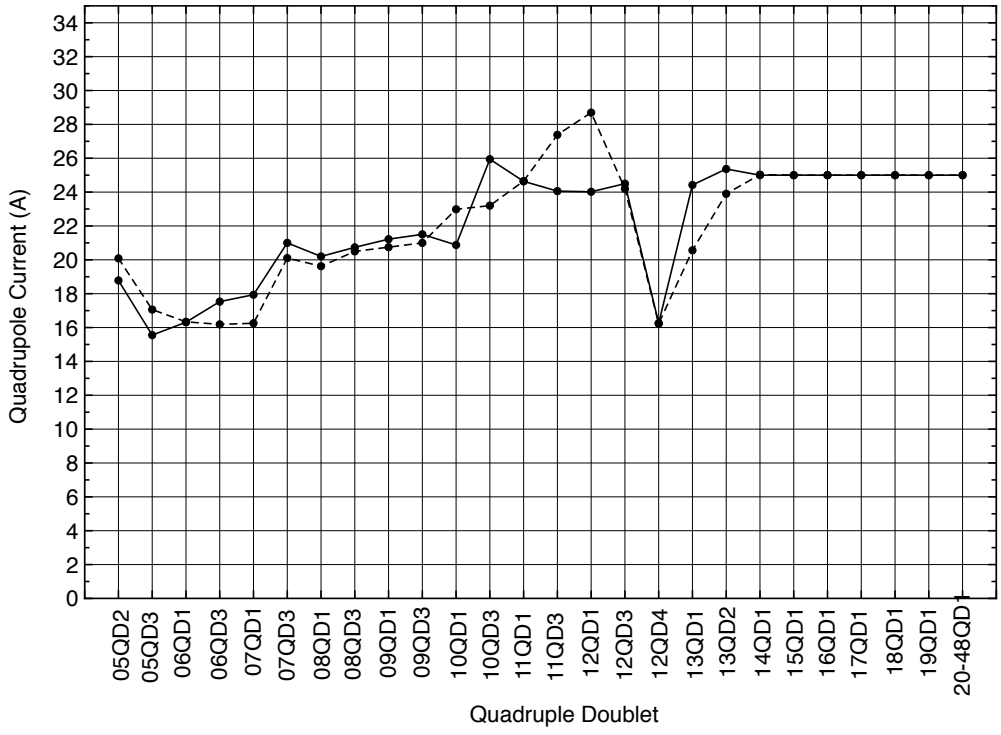

Figure 14: Quadrupole setup in 805-MHz linac: (dotted) before, (solid) after reduction of beam losses.

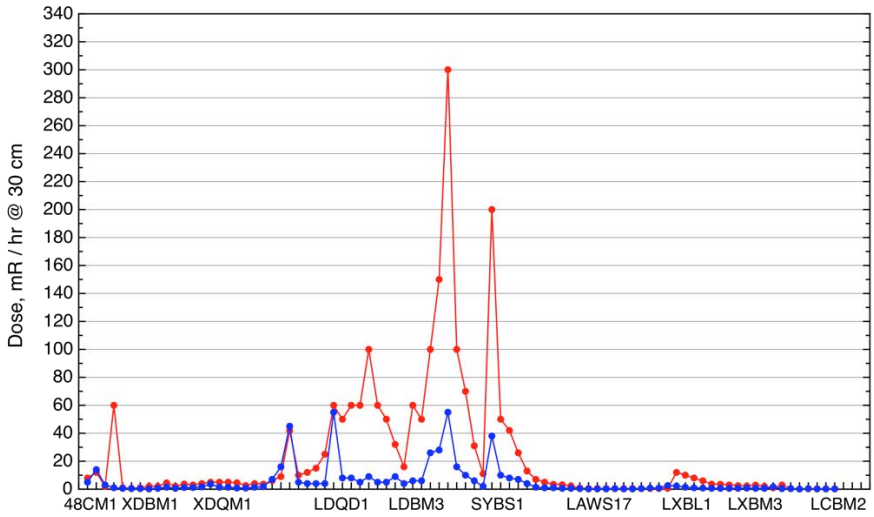

Figure 15: Switchyard radiation survey: (red) after regular tune, (blue) after improved tune.

In order to independently control tuning of the machine, phase scans, field control through klystron output power, and beam energy measurement were recently added to tuning procedure. The time-of-flight method uses absolute measurements of beam energy using direct signals from beam at an oscilloscope, as well as the difference in RF phases measured as the beam passes installed delta-t pickup loops. A newly developed BPPM data acquisition system is used [18]. Application of combined method allows tune of accelerator much more close to design with significantly reduced beam losses generated by linac in high-energy part of accelerator facility [19]. Figure 15 illustrates beam losses after 800 MeV linac in Swithyard area of accelerator facility after regular tune using only delta-t procedure, and with modified approach, using combination of phase scans, energy measurement, klystron power, and delta-t method. Application of improved tuning method resulted in significant (factor of 2) reduction of beam losses after linac.

1.1.6 **Summary**

The LANSCE is a unique accelerator facility simultaneously delivers beams to five experimental areas. Multi – beam operation requires compromise in beam tuning procedures to comply with various requirements at different target areas. Reduction of beam losses in the linac is achieved due to optimization of ion sources performance, beam-based alignment, careful tuning of the beam in each section of the accelerator facility, methodical selection of amplitudes and phases of RF tanks, control of H^- beam stripping.

1.1.7 **References**

1. K.W. Jones and P.W. Lisowski, “LANSCE High Power Operations and Maintenance Experience”, Proceedings of the Sixth International Topical Meeting on Nuclear Applications of Accelerator Technology (AccApp’03), June 1–5, 2003, p. 372–375.
2. L. Rybarcyk, “Characterizing and Controlling Beam Losses at the LANSCE

Facility", Proceedings of HB2012, Beijing, China, TUO3C03, p.324.
3. R.J. Macek, "PSR Experience with Beam Losses, Instabilities and Space Charge Effects", Workshop on space charge physics in high intensity hadron rings, AIP Conference Proceedings, Volume 448, p.p.116-127 (1998).
4. R. R. Stevens, J. R. McConnell, E. P. Chamberlin, R. W. Hamm, and R. L. York, in Proceedings of the 1979 Linear Accelerator Conference, Montauk, USA, September 10-14, (1979), p. 465.
5. Y. K. Batygin, I. N. Draganic, and C. M. Fortgang, "Experimental optimization of beam quality extracted from a duoplasmatron proton ion source", Review of Scientific Instruments, 85, 103301 (2014).
6. J. Sherman et al., AIP Conf. Proc. 763, (2005) 254.
7. B. A. Prichard, Jr. and R. R. Stevens, Jr., Los Alamos Nat. Lab. Tech. Rep. LA-UR-02-547 (2002).
8. C.Pillai et al, "Performacne of the LANSCE H- Source and Low Energy Beam Transport At Higher Peak Current", Proceedings of the 1997 Particle Accelerator Conference, Vancouver, B.C., Canada, 12-16 May 1997, 6W021. P.2743.
9. I.Kapchinsky, "Theory of Resonance Theory of Linear Resonance Accelerators", Routledge, 1985.
10. Y.K. Batygin, "Experimental improvement of 750-keV H− beam transport at LANSCE Accelerator Facility", Nuclear Inst. and Methods in Physics Research, A 904 (2018) 64–73.
11. T. Wangler, "RF Linear Accelerators", 2nd Edition, Wiley-VCH (2010).
12. M. Weiss, "Bunching of Intense Proton Beams with Six-Dimensional Matching to the Linac Acceptance," CERN/MPS/LI report 73-2 Geneva, Switzerland (1978).
13. Y.K. Batygin, "Optimization of LANSCE proton beam performance for isotope production", Nuclear Inst. and Methods in Physics Research, A 916 (2019) 8–21.
14. R.W. Garnett, E.R. Gray, L.J. Rybarcyk, and T.P. Wangler Proceedings of the 1996 Particle Accelerator Conference, p. 3185 (1996).
15. L.J. Rybarcyk, R.C. Mccrady, "The Effect of DTL Cavity Field Errors on Bema Spill at LANSCE", Proceedings of LINAC2016, East Lansing, MI, USA, MOPLR072, p.301.
16. Y.K. Batygin, "Effect of 805-MHz Linac RF Stability on Beam Losses in LANSCE High-Energy Beamlines", Proceedings of IPAC2018, Vancouver, Canada, p.1078.
17. K.R. Crandall, "The Delta-T Tuneup Procedure for the LAMPF 805-MHz Linac", LANL Report LA-6374-MS, June 1976.
18. H. Watkins, J.D. Gilpatrik, R. McCrady, Proceedings of IBIC2014, Monterey, CA, USA, WEPD09, p. 655.
19. Y.K. Batygin, F.E. Shelley, H.A. Watkins "Tuning of LANSCE 805-MHz high-energy linear accelerator with reduced beam losses", Nuclear Inst. and Methods in Physics Research, A 916 (2019) 215-225.